

## Supplemental Methods

*Generation of PGRN-deficient mice.* A targeting vector for the *Grn* locus was created with loxP sites flanking the entire *Grn* coding region, including the 3'UTR. Neomycin resistance and thymidine kinase (TK) genes were used for positive and negative selection, respectively. The vector was electroporated into RF8 (37) 129SV/Jae ESCs and positive clones were selected at a frequency of approximately 1 in 15. The positive clones were injected into C57BL/6J blastocysts to create chimeras. The chimeras were then bred with C57BL/6J females to confirm germline transmission of the *Grn*<sup>lox</sup> allele. The *Grn*<sup>lox/+</sup> mice were bred with mice expressing Cre recombinase under the  $\beta$ -actin promoter (24) to create mice that globally lack progranulin. These mice were then backcrossed with C57BL/6J mice to remove the Cre transgene. The *Grn*<sup>+/-</sup>; Cre<sup>-</sup> mice were then bred to homozygosity to generate a *Grn*-null allele. The genotyping for the *Grn*-deficient mice includes the following primers: S1 (5'-agtggggctggccacttct-3'), S2 (5'-aagattcctcgcctgggacatg-3') and AS1 (5'-gaatgctggtgctcagagggcc-3'). The *Grn*<sup>lox/lox</sup> mice were bred with mice expressing Cre recombinase under the Cd11b promoter (26) to create mice that lack progranulin in myeloid cells. All mice utilized in the paper exist on a mixed background consisting of 62.5% C57BL/6J, 12.5% 129Sv/Jae, and 25% FVB. All procedures were approved by UCSF Animal Research and followed NIH guidelines.

*Needlestick.* Three-month-old wild-type mice were anesthetized and placed on a stereotactic injection platform. A hole was drilled in the skull and a 33-gauge was inserted three times sequentially into the hippocampus. Following trauma, the scalp was closed and the mice were allowed to recover. A day later the mice were sacrificed and the

brains were collected for analysis. Mice were monitored according to IACUC protocol and received proper analgesics as needed.

*Acute MPTP treatment.* 1-methyl-4-phenyl-1,2,3,6-tetrahydropyridine (MPTP, 4  $\mu\text{g/g}$ ) or equivalent volume of PBS was injected intraperitoneally into three-month-old female mice (littermates) by four injections per day for two days. The mice were monitored according to the approved IACUC protocol and their health was scored prior to each injection. The mice were sacrificed the day after final injection and perfused with 4% PFA prior to brain extraction. The brains were post-fixed in 4% PFA overnight, followed by cryoprotection in 15% sucrose for 24 hours and then 30% sucrose for 24 hours. The brains were embedded for cryosectioning and cut into 40 $\mu\text{m}$  coronal sections. The sections containing the SNpc were stained using anti- TH (Millipore) and Iba1 (Wako) using a DAB technique (38). Stereological counting of Bregma -2.8 to -4.04 mm (6 serial sections) at 100X magnification was utilized to quantify the number of TH-, IBA1, and Nissel-positive cells in the SNpc (single hemisphere) using the StereoInvestigator Software, version 9 (MBF Bioscience) (38).

*Primary Cultures.* All cultures were grown in humidified incubators at 37°C, supplemented with 5% CO<sub>2</sub>. The ventral midbrain was harvested from E13.5 embryos as previously described (38-40). Cells from wild type ( $n=5$ ) and PGRN-deficient ( $n=4$ ) embryos were plated on six coverslips each. On day in vitro (DIV) 4, the cells were treated with vehicle, 0.2  $\mu\text{M}$ , or 0.5  $\mu\text{M}$  MPP<sup>+</sup> (in duplicate) for 3 days and then fixed in 4% PFA. Following staining, the coverslips were imaged using a Zeiss LSM confocal (40X magnification). Images were stitched together and the number of cells was quantified using ImageJ software.

Mixed cortical cultures were prepared as previously described (41). Briefly, the cortices from postnatal day 1 (P1) pups were harvested and plated on poly-L-lysine coated 12 mm coverslips (BIOCOAT) in DMEM (high glucose) supplemented with 10% FBS and penicillin/streptomycin (P/S) for eight days. On DIV5, the cultures were infected with lentivirus. On DIV8, the media was changed to Neurobasal media (Invitrogen) supplemented with N2 (Invitrogen), L-glutamine, and P/S. Four days later the conditioned media was collected and the cultures were fixed with 4% PFA. The coverslips were then stained with anti-MAP2 (Millipore), IBA1, and GFAP (Dako). ~15 images per coverslip were taken using a Leica epifluorescent microscope (40X magnification). The number of MAP2-positive cells was counted per image in order to determine the number of surviving neurons. This experiment was repeated three times.

Primary microglial cultures were obtained from cerebral cortices harvested from P2-P4 pups. The meninges were removed and the hemispheres were chopped with a razor blade and then triturated in DMEM, 20% FBS, P/S, and supplemented with 20 ng/ml GM-CSF (Peprotech). The cells were grown in poly-L-lysine coated flasks. The media was replenished three days after the initial harvest. The microglia were harvested from the astrocyte layer 6-10 days later by shaking the flasks at 200 rpm for two hours at 37°C. The media was removed and the cells were pelleted. The microglia were resuspended in Neurobasal media supplemented with N2 supplement, L-glutamine, and P/S for 24 hours prior to experimentation.

Cortical neuron cultures were prepared as previously described (29, 42). Briefly, E16-18 embryo cortices were dissected and the meninges were removed. The brains were digested with papain (Sigma). The cells were plated on 96 well plates at a density of  $0.6 \times 10^6$  cells/ml in Neurobasal media supplemented with B27 supplement (Invitrogen), L-glutamine, and P/S.

*Cytokine Analysis.* Primary microglia were harvested and cultured in Neurobasal media supplemented with L-glutamine, N2 supplement, and P/S 24 hours prior to experiments. For mRNA analysis, the cells were plated at  $1 \times 10^6$  cells/ml on 6-well plates. For secreted cytokine time course measurements, the cells were plated at  $2.5 \times 10^5$  cells/ml on 24-well plates. After 24hrs in the N2-media, control or muPGRN lentivirus was added to the cultures for 24hrs. The microglia were stimulated with PBS or 100 ng/ml LPS (Sigma) plus 100 U/ml IFN $\gamma$  (Sigma) with or without 200 ng/ml Etanercept (gift M.G. Tansey) for up to 24 hours. Conditioned media was collected for use in neuronal survival assays (6 well plates) or for ELISA (24 well plates) and the cells were lysed in Trizol (Invitrogen) for RNA extraction. Secreted cytokine levels were quantitated using the Mouse Pro-inflammatory 7-plx cytokine ELISA by Meso Scale Discovery.

*Neuron Survival Analysis.* To fluorescently label neurons, pure cortical cultures were transfected with EGFP on DIV4 using Lipofectamine2000 (Invitrogen). Following transfection, microglial conditioned media was added to the cultures. The plates were imaged every 24 hours using an automated microscopy system described by Arrasate and Finkbeiner and others (28, 29, 43, 44). Neuronal death was determined by loss of GFP fluorescence, blebbing of the soma, or neurite retraction. Kaplan-Meier and cumulative risk of death curves were generated and statistical significance was determined using the log-rank test in R. Hazard ratios between groups and conditions were calculated using Cox proportional hazards analysis in R (29).

*Real-time PCR.* RNA was harvested using Trizol (Invitrogen) according to the manufacturer's protocol from tissue (liver, kidney, brain) or cultured primary neurons and microglia. RNA (1-2 µg) was reverse-transcribed using random hexamers to generate cDNA using the SuperScript III First-Strand Synthesis System (Invitrogen). The primers used for qPCR were as follows, *Cyclo* (F 5'-tggaagagcaccaagacaaca-3', R 5'-tgccggagtgcacaatgat-3'), *progranulin* (F 5'-tggttcacacacgatgcgtttcac-3', R 5'-aaaggcaaagacactgccctgttg-3'), *Tnfa* (F 5'-acggcatggatctcaaagac-3', R 5'-agatagcaaatcggtgacg-3'), *Il1b* (F 5'-gcttcaggcaggcagtatc-3', R 5'-aggatgggctcttcttcaaag-3'), *Il10* (F 5'-agaccctcaggatgcggc-3', R 5'-ccactgccttgccttattttca). The reaction was run using the SYBR green Master Mix (QIAGEN) on an ABI Prism 7770 (Applied Biosystems). The data is normalized to the internal standard, cyclophilin, and subsequently normalized to an experimental control ( $\Delta$ CCT method, Invitrogen).

*Murine Progranulin ELISA.* Plasma was collected using a lithium heparin column (BD Biosciences) from 6-week-old mice. PGRN levels were quantified using an ELISA kit (Adipogen). Conditioned media was centrifuged to remove cellular debris. Secreted PGRN was quantified using an in-house sandwich ELISA system, using PGRN-deficient media as an internal control.

*Immunoblotting.* Frozen hemibrains were dissected into cortex, hippocampus, and cerebellum. The tissue was homogenized in RIPA buffer (Sigma) and sonicated. Conditioned media was centrifuged to remove cellular debris. Proteins were separated using the NuPage system (Invitrogen) and murine progranulin was detected using a polyclonal antibody (AF2557) (R&D Systems, Inc). Loading accuracy was determined

either by detecting tissue actin (Sigma) or Ponceau S (Sigma) to detect total protein in conditioned media.

*Immunohistochemistry/Immunocytochemistry.* Free-floating tissue sections were stained as previously described for both the DAB and fluorescent techniques (38). The following primary antibodies were incubated overnight at room temperature: TH (1:1000, Millipore), IBA1 (1:5000 Wako), GFAP (1:5000, Dako), PGRN (1:100 R&D Systems). Secondary antibodies (Vector Labs, 1:300) were incubated for 1.5 hrs at room temperature. For DAB, sections were washed with 0.1 M Tris, pH 8 and exposed to DAB solution (Vector Labs). The sections were mounted onto slides and coverslipped using Permount (Thermo Fisher Scientific) or Vectashield (Vector Labs). Images were taken at 4X magnification. Confocal images were taken using the Zeiss LSM10 (63X magnification). Cells were permeabilized with 0.1% Triton and blocked with 10% normal goat serum. The following primary antibodies were incubated overnight at 4°C: TH (1:1000, Millipore), TUJ1 (1:1000, Cell Signaling), MAP2 (1:500 Millipore). Secondary antibodies (Invitrogen) were incubated for one hour at room temperature and the slides were coverslipped using Vectashield (Vector Labs) for imaging.

## **Supplemental Results**

### **Progranulin is expressed in neurons and activated microglia in the CNS**

To investigate PGRN expression and function in the CNS, we generated PGRN-deficient mice. The murine *Grn* locus was targeted to introduce loxP sites flanking exons 2–13 (Figure S1A,B). Homozygous (*Grn*<sup>-/-</sup>) mice were generated by crossing *Grn*-floxed mice with  $\beta$ -actin-Cre mice (24). Deletion of *Grn* was verified by using quantitative PCR and immunoblotting (Figure S1C,D). Plasma levels of PGRN in *Grn*<sup>+/-</sup> mice were reduced by

~60% (Figure S1E), similar to what is seen in humans with *GRN* haploinsufficiency (45-48).

We examined PGRN expression in the adult murine brain. Immunoblotting revealed expression in the cortex, hippocampus, and cerebellum (Figure S1D). Immunohistochemical staining using a PGRN-specific antibody showed that PGRN was present mostly in neurons in various regions of the CNS, including cerebral cortex, CA1 and CA3 regions of the hippocampus, the substantia nigra pars compacta (SNpc) and ventral tegmental area (VTA) (Figure S2A). PGRN binds the scavenger receptor, *Sortilin1*, on neurons and is subsequently endocytosed (49). Therefore, immunohistochemical detection is not sufficient to determine endogenous expression versus uptake of the PGRN protein. In addition, PGRN could also be detected in non-neuronal cells, which morphologically resemble glia (Figure S2A, arrow heads). Indeed, double immunofluorescent confocal microscopy showed that PGRN co-localized with markers for microglia, but not with astrocytes (Figure S2B). We observed no PGRN staining in *Grn*<sup>-/-</sup> animals (Figure S2A)

Progranulin expression is upregulated in activated macrophages in vitro (27), in microglia following injury to the peripheral nervous system (22, 50), and in patients with neurodegenerative disease (8, 52-55). To determine whether acute expression of PGRN increases in activated CNS microglia in vivo, we induced direct traumatic injury to the cerebral cortex and hippocampus by needlestick. After 24 hours, there were increased numbers of microglia expressing increased PGRN at the injury site (Figure S2C). Thus, PGRN expression in microglia is upregulated in response to acute injury in the CNS.

## Supplemental References

37. Meiner, V.L., et al., *Disruption of the acyl-CoA:cholesterol acyltransferase gene in mice: evidence suggesting multiple cholesterol esterification enzymes in mammals*. Proc Natl Acad Sci USA, 1996. **93**(24): p. 14041-6.
38. Zhang, J., et al., *Essential function of HIPK2 in TGFbeta-dependent survival of midbrain dopamine neurons*. Nat Neurosci, 2007. **10**(1): p. 77-86.
39. Hynes, M.A., et al., *Neurotrophin-4/5 is a survival factor for embryonic midbrain dopaminergic neurons in enriched cultures*. J Neurosci Res, 1994. **37**(1): p. 144-54.
40. Farkas, L.M., et al., *Transforming growth factor-beta(s) are essential for the development of midbrain dopaminergic neurons in vitro and in vivo*. J Neurosci, 2003. **23**(12): p. 5178-86.
41. Chen, J., et al., *SIRT1 protects against microglia-dependent amyloid-beta toxicity through inhibiting NF-kappaB signaling*. J Biol Chem, 2005. **280**(48): p. 40364-74.
42. Saudou, F., et al., *Huntingtin acts in the nucleus to induce apoptosis but death does not correlate with the formation of intranuclear inclusions*. Cell, 1998. **95**(1): p. 55-66.
43. Arrasate, M. and S. Finkbeiner, *Automated microscope system for determining factors that predict neuronal fate*. Proc Natl Acad Sci U S A, 2005. **102**(10): p. 3840-5.
44. Miller, J., et al., *Quantitative relationships between huntingtin levels, polyglutamine length, inclusion body formation, and neuronal death provide*

- novel insight into huntington's disease molecular pathogenesis.* J Neurosci, 2010. **30**(31): p. 10541-50.
45. Coppola, G., et al., *Gene expression study on peripheral blood identifies progranulin mutations.* Ann Neurol., 2008. **64**(1): p. 92-6.
  46. Finch, N., et al., *Plasma progranulin levels predict progranulin mutation status in frontotemporal dementia patients and asymptomatic family members.* Brain, 2009.
  47. Ghidoni, R., L. Benussi, and G. Binetti, *Low plasma progranulin levels predict progranulin mutations in frontotemporal lobar degeneration.* Neurology, 2008. **71**(16): p. 1235-9.
  48. Sleegers, K., et al., *Serum biomarker for progranulin-associated frontotemporal lobar degeneration.* Ann Neurol., 2009.
  49. Hu, F., et al., *Sortilin-mediated endocytosis determines levels of the frontotemporal dementia protein, progranulin.* Neuron, 2010. **68**(4): p. 654-67.
  50. Naphade, S.B., et al., *Progranulin expression is upregulated after spinal contusion in mice.* Acta Neuropathol, 2010. **119**(1): p. 123-33.
  51. Baker, C.A. and L. Manuelidis, *Unique inflammatory RNA profiles of microglia in Creutzfeldt-Jakob disease.* Proc Natl Acad Sci USA, 2003. **100**(2): p. 675-9.
  52. Mackenzie, I.R.A., et al., *The neuropathology of frontotemporal lobar degeneration caused by mutations in the progranulin gene.* Brain, 2006. **129**(Pt 11): p. 3081-90.
  53. Malaspina, A., N. Kaushik, and J. de Belleruche, *Differential expression of 14 genes in amyotrophic lateral sclerosis spinal cord detected using gridded cDNA arrays.* J Neurochem, 2001. **77**(1): p. 132-45.

54. Philips, T., et al., *Microglial Upregulation of Progranulin as a Marker of Motor Neuron Degeneration*. *J Neuropathol Exp Neurol*, 2010. **69**(12): p. 1191-1200.

**Supplemental Table S1.**

Neuron Genotype	Media	N	HR	p
<i>Grn</i> <sup>+/+</sup>	Neurobasal + B27	744	Ref	
<i>Grn</i> <sup>-/-</sup>	Neurobasal + B27	1137	1.17	0.008
<i>Grn</i> <sup>+/+</sup>	Neurobasal + N2	513	Ref	
<i>Grn</i> <sup>-/-</sup>	Neurobasal + N2	426	1.21	0.007

**Table S1. Progranulin-deficiency affects cortical neuron survival in vitro.** Hazard ratios (HR) were determined for populations of neurons over time to indicate alterations in survival. Progranulin-deficient primary cortical neurons cultured in the absence of glia have decreased survival. HR, hazard ratio.

### Supplemental Figure Legends

**Figure S1. Generation of progranulin-deficient mice.** (A) Generation of the targeting vector with loxP sequences flanking the entire *Grn* coding region (black boxes represent coding exons). Black triangles, loxP sites; grey triangles, FRT sites; grey box, neomycin-resistance cassette (neo); white box, thymidine kinase (TK). Primers for the genotyping reaction are denoted with black arrows. Key restriction enzyme sites are indicated (N, *NotI*; E, *EcoRI*). (B) PCR genotyping results for *Grn*-deficient mice after crossing with mice expressing Cre under the  $\beta$ -actin promoter. (C) Relative *Grn* mRNA expression in brain, liver, and kidney of 6-week-old PGRN-deficient mice. (ND, not detected). \*p < 0.001. (D) PGRN protein levels evaluated with immunoblotting of liver, kidney, brain,

and plasma samples taken from 6-week-old PGRN-deficient mice. **(E)** PGRN protein levels found in the plasma of 6-week-old PGRN-deficient mice detected using ELISA. (ND, not detected). Total refers to data from both sexes combined (M, male; F, female). \* $p < 0.001$ .

**Figure S2. Progranulin expression in the CNS. (A)** Immunohistochemistry showing the presence of PGRN in neurons of the frontal cortex, hippocampus, and substantia nigra pars compacta (SNpc). Boxes indicate area imaged at higher magnification shown in the inset images. Arrow heads highlight detection of PGRN in non-neuronal cells. VTA, ventral tegmental area. Bar = 1200  $\mu\text{m}$ . **(B)** Confocal images showing that in addition to neurons, PGRN protein can be detected in microglia, but not astrocytes. The inset box in the merged image depicts the cell imaged at higher magnification to demonstrate co-localization of PGRN expression. Bar = 20  $\mu\text{m}$ . **(C)** PGRN expression is upregulated in microglia 24 hours following a needlestick trauma to the hippocampus. Activated microglia (morphology-inset) are present in the area of the needle track in both wild type and PGRN-deficient mice compared with the contralateral, uninjured hemisphere. These activated microglia have upregulated PGRN expression (inset) that is not present in the PGRN-deficient brains. Bar = 1200  $\mu\text{m}$ .

**Figure S3. Death of all neuronal populations in the SNpc following MPTP treatment. (A)** Representative SNpc sections showing decreased numbers of Nissl-positive neurons following MPTP exposure in PGRN-deficient mice compared to control. Dashed lines denote the SNpc. Bar = 500  $\mu\text{m}$ . **(B)** Quantification of Nissl-positive neurons in the SNpc. Numbers indicate the  $n$  per group. \* $p < 0.05$  PBS compared with MPTP. † $p < 0.05$   $Grn^{+/+}$  MPTP compared with  $Grn^{-/-}$  MPTP.

**Figure S4. Efficiency and phenotype of *Cd11b-Cre* mice following MPTP treatment.**

(A) Graph showing *Grn* mRNA levels in microglia and cortical neurons *in vitro*. \* $p < 0.001$  *Cd11b-Cre*<sup>-</sup>;*Grn*<sup>fllox/fllox</sup> compared with *Cd11b-Cre*<sup>+</sup>;*Grn*<sup>fllox/fllox</sup> cells. (B) Quantification of secreted PGRN levels in microglial cultures. \* $p < 0.01$  *Cd11b-Cre*<sup>-</sup>;*Grn*<sup>fllox/fllox</sup> compared with *Cd11b-Cre*<sup>+</sup>;*Grn*<sup>fllox/fllox</sup> microglia. (C) Representative SNpc sections showing decreased numbers of TH-positive neurons following MPTP treatment in *Cd11b-Cre*<sup>+</sup>;*Grn*<sup>fllox/fllox</sup> mice. VTA, ventral tegmental region; dashed lines denote the SNpc. Bar= 500  $\mu$ m. (D) Representative images showing increased microgliosis in *Cd11b-Cre*<sup>+</sup>;*Grn*<sup>fllox/fllox</sup> mice treated with MPTP demonstrated by Iba1 staining. Dashed circle and arrow denote the SNpc. Bar = 500  $\mu$ m.

**Figure S5. Murine PGRN lentiviral infection restores PGRN expression in**

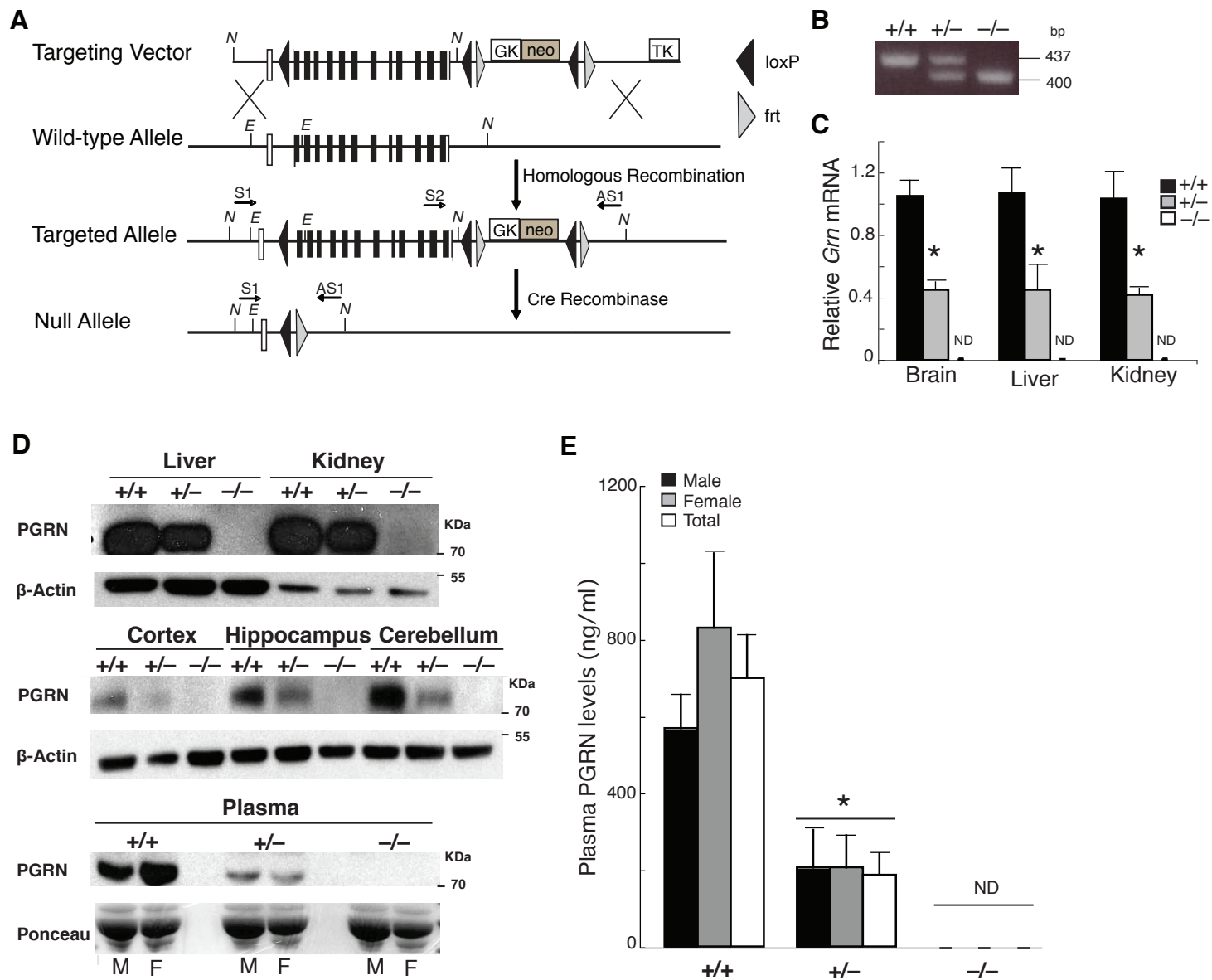
**microglia.** (A) Quantification of secreted PGRN from microglia infected with either murine PGRN or control lentivirus and LPS/IFN $\gamma$  stimulation. \* $p < 0.001$  compared with WT PBS control infected microglia. (B) Graph showing *Grn* mRNA levels following infection with either a murine PGRN or control lentivirus and LPS/IFN $\gamma$  stimulation. \* $p < 0.05$  compared with KO PBS.

**Figure S6. Depletion of TNF $\alpha$  using Etanercept is not sufficient to rescue cytotoxic**

**neuronal death *in vitro*.** Wild type neurons exposed to conditioned media from LPS/IFN $\gamma$ -treated PGRN-deficient microglia had an increased risk of death that is not attenuated by depletion of TNF $\alpha$  by co-treatment with Etanercept. \* $p < 0.01$  (log-rank test), WT PBS compared with KO PBS. \*\* $p < 0.0001$  (log-rank test), LPS/IFN $\gamma$ -treated microglial conditioned media compared with PBS treated conditioned media.

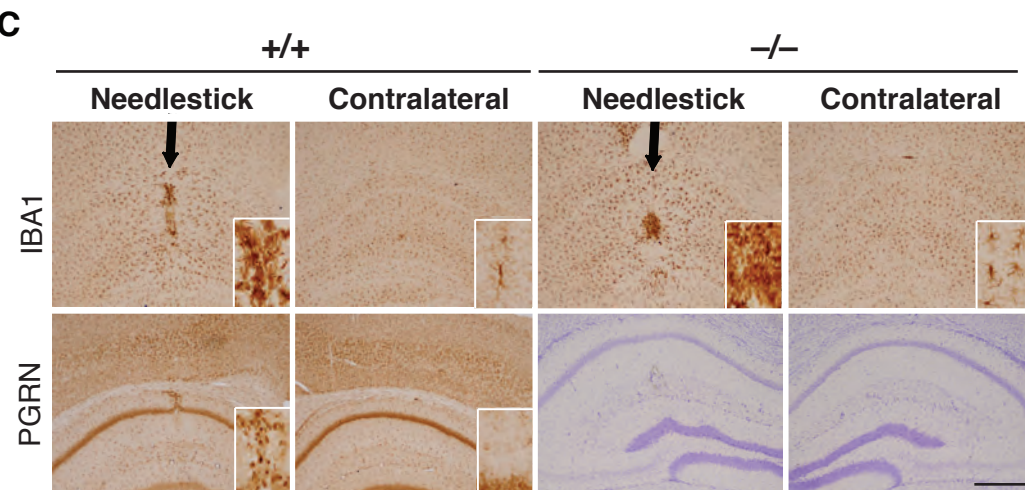
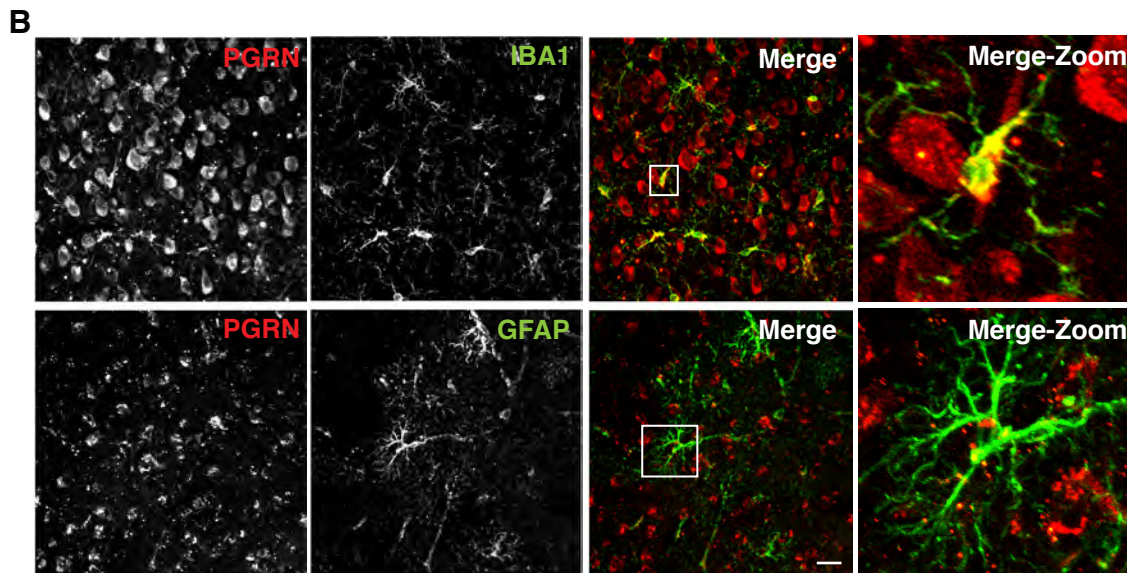
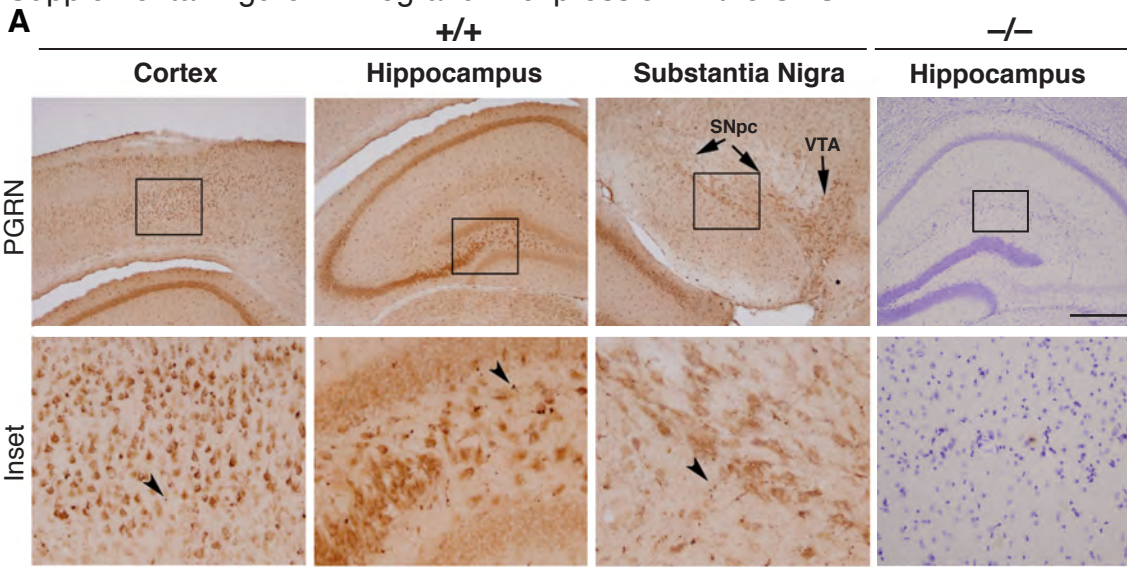


Supplemental Figure 1. Generation of progranulin-deficient mice.

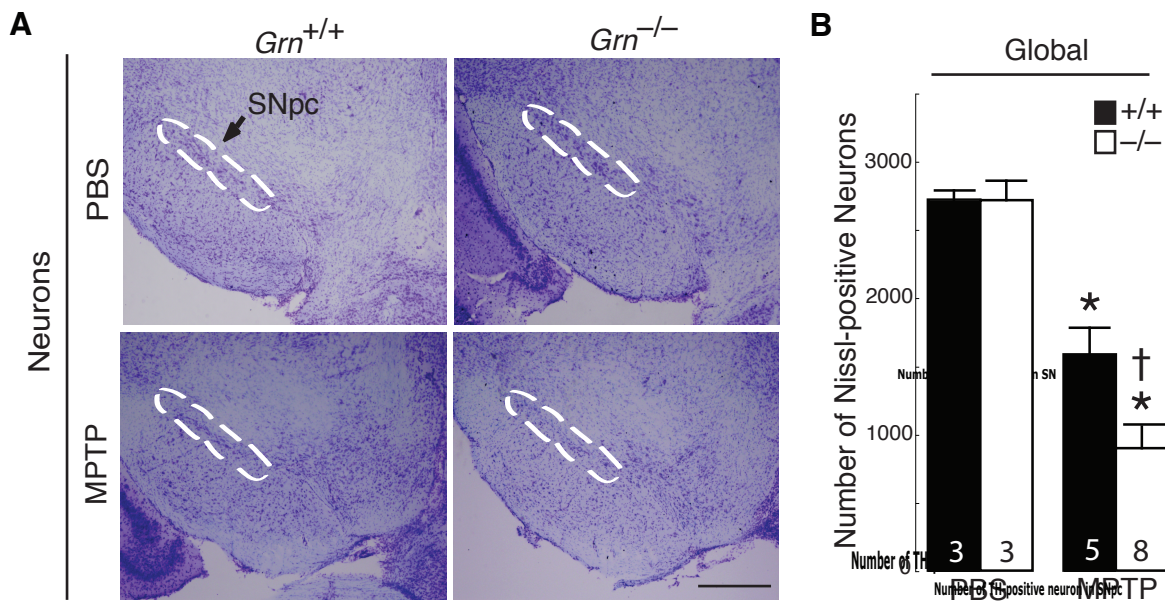


**Figure S1. Generation of progranulin-deficient mice.** (A) Generation of the targeting vector with loxP sequences flanking the entire *Grn* coding region (black boxes represent coding exons). Black triangles, loxP sites; grey triangles, FRT sites; grey box, neomycin-resistance cassette (*neo*); white box, thymidine kinase (*TK*). Primers for the genotyping reaction are denoted with black arrows. Key restriction enzyme sites are indicated (N, *NotI*; E, *EcoRI*). (B) PCR genotyping results for *Grn*-deficient mice after crossing with mice expressing Cre under the  $\beta$ -actin promoter. (C) Relative *Grn* mRNA expression in brain, liver, and kidney of 6-week-old PGRN-deficient mice. (ND, not detected). \* $p < 0.001$ . (D) PGRN protein levels evaluated with immunoblotting of liver, kidney, brain, and plasma samples taken from 6-week-old PGRN-deficient mice. (E) PGRN protein levels found in the plasma of 6-week-old PGRN-deficient mice detected using ELISA. (ND, not detected). Total refers to data from both sexes combined (M, male; F, female). \* $p < 0.001$ .

Supplemental Figure 2. Progranulin expression in the CNS.

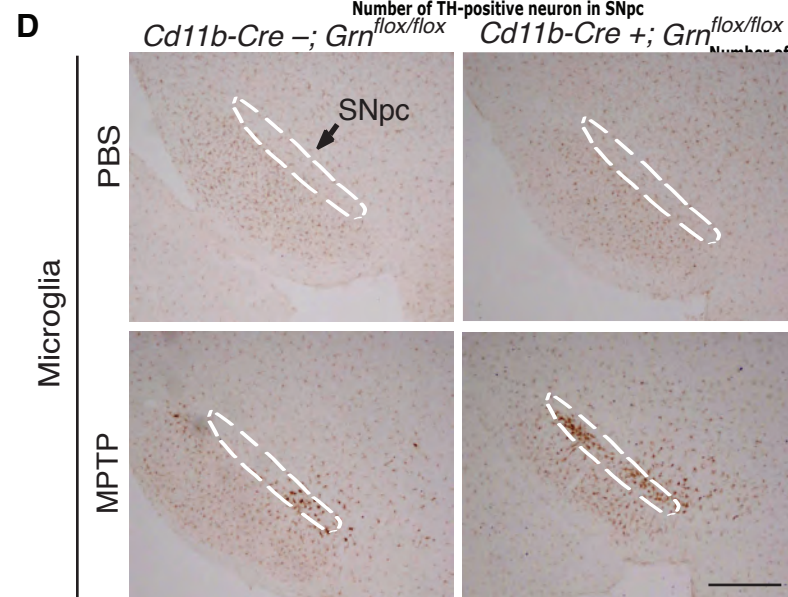
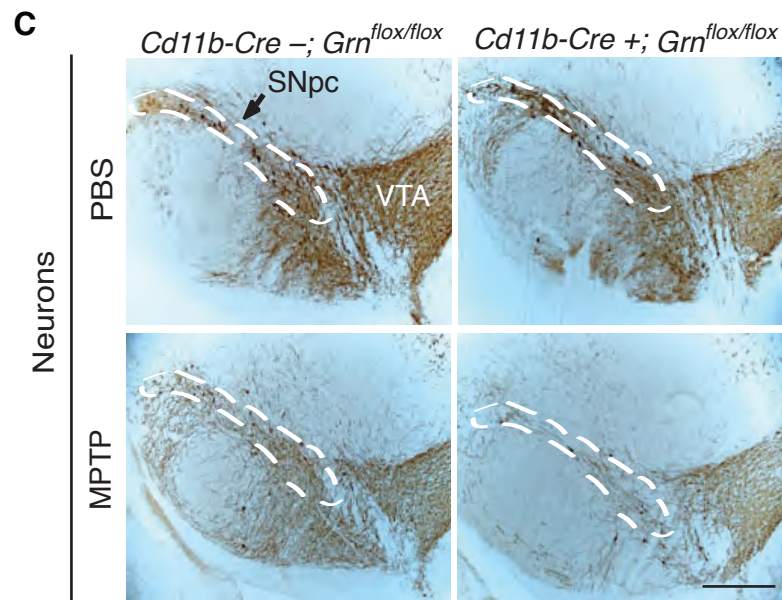
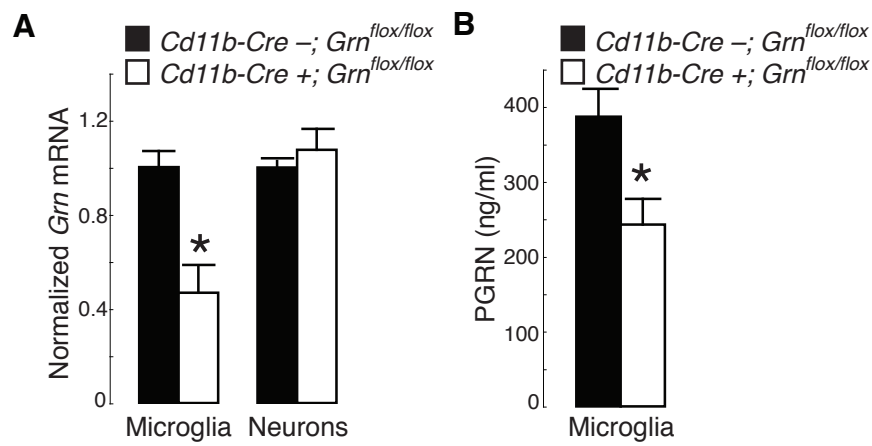


**Figure S2. Progranulin expression in the CNS.** (A) Immunohistochemistry showing the presence of PGRN in neurons of the frontal cortex, hippocampus, and substantia nigra pars compacta (SNpc). Boxes indicate area imaged at higher magnification shown in the inset images. Arrow heads highlight detection of PGRN in non-neuronal cells. VTA, ventral tegmental area. Bar = 1200  $\mu$ m. (B) Confocal images showing that in addition to neurons, PGRN protein can be detected in microglia, but not astrocytes. The inset box in the merged image depicts the cell imaged at higher magnification to demonstrate co-localization of PGRN expression. Bar = 20  $\mu$ m. (C) PGRN expression is upregulated in microglia 24 hours following a needlestick trauma to the hippocampus. Activated microglia (morphology-inset) are present in the area of the needle track in both wild type and PGRN-deficient mice compared with the contralateral, uninjured hemisphere. These activated microglia have upregulated PGRN expression (inset) that is not present in the PGRN-deficient brains. Bar = 1200  $\mu$ m.



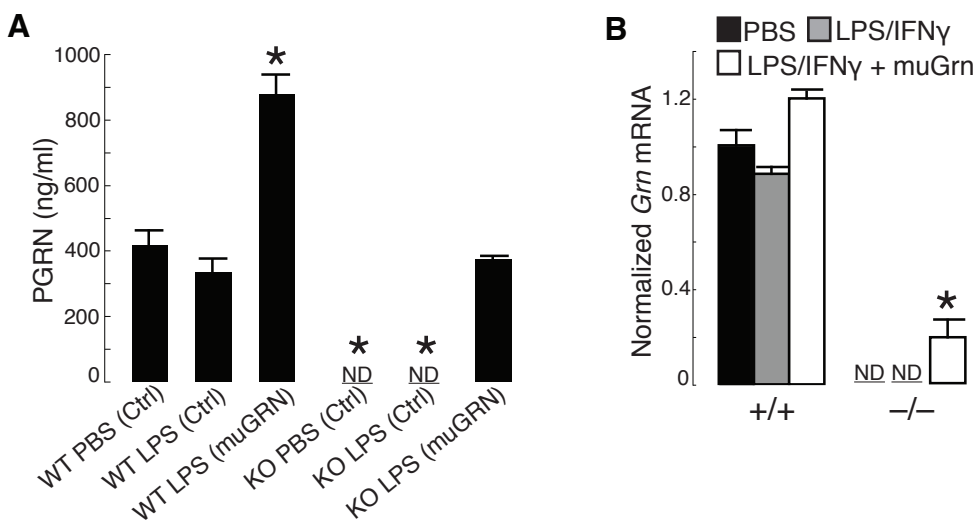
**Figure S3. Death of all neuronal populations in the SNpc following MPTP treatment. (A)** Representative SNpc sections showing decreased numbers of Nissl-positive neurons following MPTP exposure in PGRN-deficient mice compared to control. Dashed lines denote the SNpc. Bar = 500  $\mu$ m. **(B)** Quantification of Nissl-positive neurons in the SNpc. Numbers indicate the *n* per group. \**p* < 0.05 PBS compared with MPTP. †*p* < 0.05 *Grn*<sup>+/+</sup> MPTP compared with *Grn*<sup>-/-</sup> MPTP.

Figure S4. Martens et al.



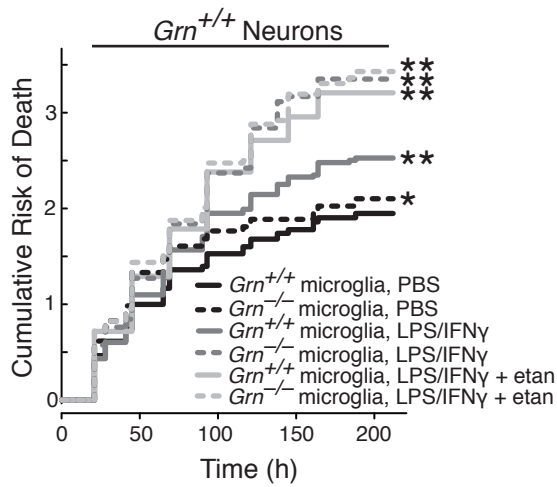
**Figure S4. Efficiency and phenotype of Cd11b-Cre mice following MPTP treatment. (A)** Graph showing *Grn* mRNA levels in microglia and cortical neurons in vitro. \* $p < 0.001$  *Cd11b-Cre*<sup>-</sup>; *Grn*<sup>flox/flox</sup> compared with *Cd11b-Cre*<sup>+</sup>; *Grn*<sup>flox/flox</sup> cells. **(B)** Quantification of secreted PGRN levels in microglial cultures. \* $p < 0.01$  *Cd11b-Cre*<sup>-</sup>; *Grn*<sup>flox/flox</sup> compared with *Cd11b-Cre*<sup>+</sup>; *Grn*<sup>flox/flox</sup> microglia. **(C)** Representative SNpc sections showing decreased numbers of TH-positive neurons following MPTP treatment in *Cd11b-Cre*; *Grn*<sup>flox/flox</sup> mice. VTA, ventral tegmental area; dashed lines denote the SNpc. Bar = 500  $\mu$ m. **(D)** Representative images showing increased microgliosis in *Cd11b-Cre*<sup>+</sup> *Grn*<sup>flox/flox</sup> mice treated with MPTP demonstrated by IBA1 staining. Dashed circle and arrow denote the SNpc. Bar = 500  $\mu$ m.

Figure S5. Martens et al.



**Figure S5. Murine PGRN lentiviral infection restores PGRN expression in microglia.** (A) Quantification of secreted PGRN from microglia infected with either murine PGRN or control lentivirus and LPS/IFN $\gamma$  stimulation. \*p < 0.001 compared with WT PBS control infected microglia. (B) Graph showing *Grn* mRNA levels following infection with either a murine PGRN or control lentivirus and LPS/IFN $\gamma$  stimulation. \*p < 0.05 compared with KO PBS.

Figure S6. Martens et al.



**Figure S6. Depletion of TNF $\alpha$  using Etanercept is not sufficient to rescue cytotoxic neuronal death in vitro.** Wild type neurons exposed to conditioned media from LPS/IFN $\gamma$ -treated PGRN-deficient microglia had an increased risk of death that is not attenuated by co-treatment with Etanercept. \* $p < 0.01$  (log-rank test), WT PBS compared with KO PBS. \*\* $p < 0.0001$  (log-rank test), LPS/IFN $\gamma$ -treated microglial conditioned media compared with PBS treated conditioned media.